

# Thermodynamics of spin systems on small-world hypergraphs

D. Bolle, R. Heylen and N.S. Skantzos

Katholieke Universiteit Leuven, Instituut voor Theoretische Fysica, Celestijnenlaan 200D, B-3001 Leuven, Belgium

We study the thermodynamic properties of spin systems on small-world hypergraphs, obtained by superimposing sparse Poisson random graphs with p-spin interactions onto a one-dimensional Ising chain with nearest-neighbor interactions. We use replica-symmetric transfer-matrix techniques to derive a set of fixed-point equations describing the relevant order parameters and solve them employing population dynamics. In the limit of a fully connected graph part, we are able to solve for the order parameters analytically. We determine the ferromagnetic-paramagnetic phase transition lines for all values of p and different long-range connectivities. These results are compared with extensive Monte-Carlo simulations. In particular, we find very good agreement for ferromagnetic interactions. For anti-ferromagnetic interactions critical slowing down near the transition lines does occur.

PACS numbers: 64.60.Cn, 05.20.-y, 89.75.-k

## I. INTRODUCTION

In recent years, a large amount of work has been devoted to the study of small-world networks, mainly numerical [1] with emphasis e.g. on biophysical networks [2]-[4] or social networks [5] and, to a lesser extent, analytically [6, 7]. For recent reviews see e.g. [8]-[12]. By now, it has thus become apparent that small-world architectures can be found in many different circumstances, ranging from linguistic, epidemic and social networks to the world-wide-web.

Scientific modeling of real-world applications not only often requires a diluted random graph to describe the interactions but, moreover, in many cases more than two agents interact with each other. In that case a simple edge-vertex description is no longer sufficient. A model that incorporates these features is the diluted random graph with p-spin interactions. In this context, a ferromagnetic model having 3-spin interactions and finite connectivity has been considered recently in [13]. (See also [14, 15]).

A complete description of a small-world system requires in addition local interactions. A simple example of the latter is the nearest-neighbor ferromagnetic Ising interaction. The inclusion of such local interactions can completely change the functioning and the dynamics of such systems. It was shown in [7], e.g., that this construction significantly enlarges the region in parameter space where ferromagnetism occurs. In particular, the ferromagnetic-paramagnetic transition occurs at a finite temperature for any value of the average long-range connectivity, however small. Furthermore, a jump in the entropy of metastable configurations has been found [16] exactly at the crossover between the small-world and the Poisson random graph structure due to the formation of disconnected clusters within the graph.

In this work we study the thermodynamic properties of such a small-world hypergraph, obtained by superimposing sparse Poisson random graphs with p-spin interactions onto a one-dimensional Ising chain with nearest-neighbor interactions. An analytic study of this model is non-trivial. The relevant disorder-averaged free energy and order parameters are calculated using replica-symmetric transfer-matrix techniques. A set of fixed-point equations for the order parameter functions is derived and solved numerically with the population dynamics algorithm [17]. For  $p = 2$  we find back some of the results described in [7], [18, 19], for  $p = 3$  the physics is different. In the limit of a fully connected graph part, we get a mean-field model for which we are able to solve the order parameters in a completely analytic way, again using transfer matrices. First-order phase transitions from the ferromagnetic to the paramagnetic phase are found for all values of p. Additionally, for  $p = 2$  a second-order phase transition and a coexistence region between the two phases are found.

These results are compared with extensive Monte-Carlo simulations using Glauber dynamics. Very good agreement with the theory is found when the Ising chain interactions are ferromagnetic. When they are anti-ferromagnetic we find that the dynamics becomes very slow, indicating critical slowing down near the transition lines.

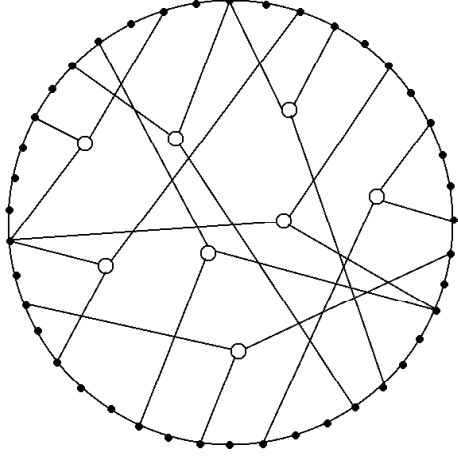


FIG. 1: Schematic representation of a hypergraph of degree 3 superimposed onto an Ising chain. Each black dot represents a spin, where each circle represents a hyperedge involving 3 spins

The rest of this paper is organized as follows. In Sec. II we define the small-world model. In Sec. IIIA we derive the saddle-point equations for the relevant order parameter function. Sec. IIIB discusses the transfer-matrix analysis in the replica symmetric approximation leading to a set of fixed-point equations involving the eigenvectors. Expressions for the free energy and the physical order parameters are given in Sec. IIIC. There, we also discuss the continuous bifurcations from zero magnetization. Sec. IV gives the analytic solution of the fully connected version of the model. In Sec. V we numerically study the fixed-point equations and compare the results with simulations. Finally, Sec. VI contains the concluding remarks.

## II. THE MODEL

Consider a system of  $N$  Ising spins  $\sigma = (\sigma_1; \dots; \sigma_N)$ , with  $\sigma_i \in \{-1, 1\}$ , arranged on a one-dimensional chain ( $\sigma_{N+1} = \sigma_1$ ). Two different couplings are assumed to be present in this system: first, nearest-neighbor interactions of uniform strength  $J_0$  and, secondly, sparse long-range  $p$ -spin interactions of the form  $c_{j_1; \dots; j_p}$ ,  $j_1 < j_2 < \dots < j_p$ , of uniform strength  $J$ , which can be described by an hypergraph of degree  $p$ . An example of such a system for  $p = 3$  is shown in Fig. 1.

The couplings  $c_{j_1; \dots; j_p}$  are independent identically distributed random variables, for  $j_1 < j_2 < \dots < j_p$ , taken from the following distribution

$$P(c_{j_1; \dots; j_p}) = c \frac{(p-1)!}{N^{p-1}} c_{j_1; \dots; j_p; 1} + (1 - c) \frac{(p-1)!}{N^{p-1}} c_{j_1; \dots; j_p; 0} \quad (1)$$

The value  $c_{j_1; \dots; j_p} = 1$  indicates that the hyperedge formed by the  $p$  spins  $(\sigma_{j_1}; \dots; \sigma_{j_p})$  is present, whereas  $c_{j_1; \dots; j_p} = 0$  means that there is no such hyperedge present. The quantity  $c$  indicates the total number of hyperedges a spin is, on average, part of

$$\frac{1}{N} \sum_{\substack{i < j_1 < \dots < j_p \\ i \in \{1, \dots, N\}}} c_{i; j_1; \dots; j_p; 1} = c \quad (2)$$

In the small-world context one takes  $c$  to be a small number of order  $O(1)$  while  $c \ll 1$ .

We assume that the couplings are symmetric such that for any permutation  $\pi$  in  $S_p$

$$c_{j_1; \dots; j_p} = c_{j_{\pi(1)}; \dots; j_{\pi(p)}} \quad (3)$$

Furthermore, we exclude self-interactions and hyperedges of reduced degree by stating that

$$8k \in 12 f1; ::::; pg : j_k = j_1) \quad c_{j_1 :::: j_p} = 0 \quad (4)$$

meaning that the hyperedge does not exist when any two indices are equal.

At thermal equilibrium, such a system can be described by the Hamiltonian

$$H(\cdot) = \sum_i h_i(\cdot) \quad (5)$$

where the local  $\text{eld}$  consists out of a hypergraph part and a chain part.

$$h_i(x) = \frac{J}{\Phi} \sum_{j_1 < \dots < j_{p-1}} c_{i, j_1, \dots, j_{p-1}} x_{j_1} \dots x_{j_{p-1}} + \frac{J_0}{2} (x_{i-1} + x_{i+1}) \quad (6)$$

We want to study the thermodynamic properties of this network structure. In the next Section we derive the relevant saddle-point equations starting from the free energy of the system.

### III. REPLICATED TRANSFER-MATRIX ANALYSIS

### A . Saddle-point equations

We start from the free energy of the system written down in the replica approach [20]

$$f(\ ) = \lim_{N \rightarrow \infty} \lim_{n \rightarrow \infty} \frac{1}{n!} \log \frac{1}{n!} \prod_{i=1}^n i^{\frac{1}{i}} \quad (7)$$

$$hZ^n i_C = \exp \left( \sum_{k=1}^n \frac{1}{k} \frac{d}{dt} \right) H(t) \Big|_{t=0} \quad (8)$$

with  $\tau = 1, \dots, n$  the replica index and the average taken over all possible graphs  $c$  according to the distribution (1), so that we obtain

$$hZ^n i_C = \frac{X}{1 - \exp \left( \frac{X}{J_0} \right)} \frac{1}{i_{i+1} A} \frac{Y}{1 - \exp \left( \frac{X}{\frac{J}{C}} \right)} \frac{*}{i_{i+1} j_1; \dots; j_{p-1} j_1 \dots j_{p-1}} ! + \dots \quad (9)$$

$$= \frac{\prod_{i=1}^n \frac{1}{i!} \prod_{i=1}^p \frac{(p-1)!}{(N-p+1)!} \prod_{j_1 < \dots < j_p} \frac{1}{j_1! \dots j_p!}}{\prod_{i=1}^n \prod_{i=1}^p \frac{1}{i!} \prod_{j_1 < \dots < j_p} \frac{1}{j_1! \dots j_p!}} \exp \left( \sum_{i=1}^p \frac{c}{N} \right) \quad (10)$$

where we have used the fact that  $N$  is large to contract the average over  $c_{1,1}, \dots, c_{N,N}$  into an exponential.

The next step is to insert unities  $1 = \dots$ ;  $i$  and  $1 = \dots$ ;  $j$  where  $\dots$  are auxiliary vectors in replica space to arrive at

$$hZ^n i_C = \frac{X}{1+i_1} \exp @ \frac{X}{J_0} \frac{1}{i_1} \dots \frac{1}{i_{p-1}} A \exp @ \frac{c}{pN^{p-1}} \frac{X}{1+i_p} \dots \frac{X}{i_k} A \dots \frac{X}{i_{p-1}} A \dots \frac{1}{i_p} A \quad (11)$$

In this way we have effectively introduced an order function

$$F(\cdot) = \frac{1}{N} \sum_i^N \cdot_i \quad ; \quad i = 1, 2, \dots, N \quad (12)$$

that can be inserted in (11) in the usual way

$$1 = \frac{1}{N} \sum_{i=1}^N \exp \left[ -\frac{1}{2} \left( \frac{F(\hat{F}^{-1}(X_i)) - F(X_i)}{\sigma} \right)^2 \right] \quad ; \quad (13)$$

to obtain

We can then apply the saddle-point method resulting in

$$\begin{aligned}
 \log(hZ^n i_C) = & \underset{\substack{X \\ F \neq F}}{\text{Extr}^{\theta}} \underset{i}{X} \underset{\substack{Y^p \\ F(-k)}}{F(-)} + \frac{c}{p} \underset{\substack{X \\ 1 \dots p}}{\underset{k=1}{\dots}} \underset{\substack{Y^p \\ F(-k)}}{F(-k)} e^{\frac{-j}{c} p} \dots_1 \dots_p \underset{1}{1} \\
 & + \frac{1}{N} \log \underset{\substack{X \\ 1 \dots n}}{4} \exp \underset{i}{J_0} \underset{\substack{X \\ i \dots i+1}}{i} \underset{i}{F(-i)} 5A
 \end{aligned} \quad (15)$$

Derivation with respect to  $F(\cdot)$  and  $\hat{F}(\cdot)$  leads to the following equations

$$\hat{F}(\ ) = \frac{1}{iC} \frac{X}{F(k)} e^{\frac{J}{C}P} \dots \frac{1}{P-1} \quad (16)$$

$$F(\ ) = \frac{1}{N} \frac{1 \dots p_1 k=1}{P} \frac{h_P}{P} \frac{i}{exp} \frac{J_0}{P} \frac{P}{j} \frac{j}{j+1} \frac{P}{i} \frac{j}{j} \hat{F}(\ ) \quad (17)$$

and using (16) to remove  $\hat{F}(\cdot)$  results in a self-consistent equation for the density  $F(\cdot)$ :

$$F(\cdot) = \frac{P \cdot \frac{h}{N} \cdot P \cdot i \cdot \exp \left( J_0 \cdot \frac{P}{j} \cdot j + C \cdot \frac{P}{j} \cdot j + \frac{Q}{k=1} \cdot \frac{p}{k} \cdot F(k) \cdot e^{-\frac{J}{c} \cdot P} \right) \cdot 1 \cdots p \cdot 1 \cdot j \cdot 1}{P \cdot \exp \left( J_0 \cdot \frac{P}{j} \cdot j + C \cdot \frac{P}{j} \cdot j + \frac{Q}{k=1} \cdot \frac{p}{k} \cdot F(k) \cdot e^{-\frac{J}{c} \cdot P} \right) \cdot 1 \cdots p \cdot 1 \cdot j \cdot 1} \quad (18)$$

## B. Transfer-m atrix analysis

Defining the following  $2^n \times 2^n$  matrix

$$T, \mathbb{F} = \exp @ J_0^X + c X \mathbb{F}^1_{(k)} e^{-\frac{J}{c} P} \dots_{p-1}^1 A \quad (19)$$

Eq. (18) reads

$$F(\lambda) = \frac{\frac{1}{N} \sum_{j=1}^{N-1} T^{j-1} [F]_{j,j+1}}{\text{tr}(T^N [F])} \quad (20)$$

We insert unity  $1 = P_j$ ; and introduce the matrix  $Q_j(\lambda) = \lambda P_j - Q_j$ ; to obtain after some algebra

$$F(\cdot) = \frac{\text{tr}(T^N F P(\cdot))}{\text{tr}(T^N F)} \quad (21)$$

To proceed with the evaluation of the traces in (21) we remark that in the thermodynamic limit  $N \rightarrow \infty$  only the largest eigenvalue of  $T^N F$  will contribute. Using

$$\mathbb{E}^X_T [F] u(\cdot) = \mathbb{E}_0 u(\cdot) \quad (22)$$

$$\mathbb{E}^X_T [v(\cdot) F] = \mathbb{E}_0 v(\cdot) \quad (23)$$

we have that

$$\mathbb{E}^X_T [F] = \mathbb{E}_0 u(\cdot) v(\cdot) \quad (24)$$

and consequently

$$F(\cdot) = \frac{\mathbb{E}_0 u(\cdot) v(\cdot)}{\mathbb{E}_0 u(\cdot) v(\cdot)} \quad (25)$$

So, in order to find a solution for  $F(\cdot)$  we need to solve the eigenvector equations (22) and (23).

At this point we invoke replica symmetry (RS) by assuming that  $\mathbb{E}^X_T [F] = F(\langle x \rangle)$ . One way to fulfill this is to write  $F(\cdot)$  as follows [17]

$$F(\cdot) = \frac{Z}{\int dh W(h)} \frac{Y^n}{\sum_{h=1}^Z \frac{e^h}{2 \cosh(h)}} \quad (26)$$

The density  $W(h)$  is normalized. We also assume the left and right eigenvectors to be replica symmetric

$$u(\cdot) = \frac{Z}{dx} \langle x \rangle \frac{Y^n}{\sum_{x=1}^Z e^x} \quad (27)$$

$$v(\cdot) = \frac{Z}{dy} \langle y \rangle \frac{Y^n}{\sum_{y=1}^Z e^y} \quad (28)$$

This allows us to write down self-consistent equations for  $\langle x \rangle$  and  $\langle y \rangle$ . We insert Eqs. (26) and (27) into the l.h.s. of Eq. (22) and obtain after some tedious algebra (see the Appendix for more details) the following closed equation for  $\langle x \rangle$

$$\langle x \rangle = \frac{\frac{X}{Z} \frac{e^{-cC}}{!} \sum_{k=1}^n \frac{Y}{\tanh(\frac{J}{c} \sum_{k=1}^n \tanh(\tanh(\frac{J}{c} \sum_{k=1}^n \tanh(h_k))) + \tanh(\tanh(x) \tanh(J_0)))}}{\int dh_k W(h_k)} \quad (\#)$$

$$\langle x \rangle = \frac{\frac{X}{Z} \frac{e^{-cC}}{!} \sum_{k=1}^n \frac{Y}{\tanh(\tanh(\frac{J}{c} \sum_{k=1}^n \tanh(h_k))) + \tanh(\tanh(x) \tanh(J_0)))}}{\int dh_k W(h_k)} \quad (\#\#)$$

$$\langle x \rangle = \frac{\frac{X}{Z} \frac{e^{-cC}}{!} \sum_{k=1}^n \frac{Y}{\tanh(\tanh(\frac{J}{c} \sum_{k=1}^n \tanh(h_k))) + \tanh(\tanh(x) \tanh(J_0)))}}{\int dh_k W(h_k)} \quad (29)$$

In a similar way we derive a self-consistent equation for  $\langle y \rangle$  by inserting (26) and (28) into the l.h.s. of Eq. (23)

$$\langle y \rangle = \frac{\frac{Y}{Z} \frac{e^{-cC}}{!} \sum_{k=1}^n \frac{X}{\tanh(\tanh(\frac{J}{c} \sum_{k=1}^n \tanh(h_k))) + \tanh(\tanh(x) \tanh(J_0)))}}{\int dy_k W(y_k)} \quad (\#)$$

$$\langle y \rangle = \frac{\frac{Y}{Z} \frac{e^{-cC}}{!} \sum_{k=1}^n \frac{X}{\tanh(\tanh(\frac{J}{c} \sum_{k=1}^n \tanh(h_k))) + \tanh(\tanh(x) \tanh(J_0)))}}{\int dy_k W(y_k)} \quad (\#\#)$$

$$\langle y \rangle = \frac{\frac{Y}{Z} \frac{e^{-cC}}{!} \sum_{k=1}^n \frac{X}{\tanh(\tanh(\frac{J}{c} \sum_{k=1}^n \tanh(h_k))) + \tanh(\tanh(x) \tanh(J_0)))}}{\int dy_k W(y_k)} \quad (30)$$

At this point we choose the  $\langle x \rangle$  and  $\langle y \rangle$  to be normalized.

Next, to find the self-consistent equation for  $W(h)$  we start from Eq. (25) and fill in the RS-assumptions (27) and (28). In the limit  $N \rightarrow \infty$  we identify the result with Eq. (26) and we get

$$W(h) = \frac{1}{Z} \int dx dy \langle x \rangle \langle y \rangle (h - x - y) \quad (31)$$

Finally, in order to calculate the free energy we need to determine the largest eigenvalue  $\lambda_0$  in the limit  $n \rightarrow 0$ . We start from Eq. (22), insert Eqs. (26) and (27) to obtain

$$\lambda_0 = 1 + n \frac{\frac{X}{2} \frac{e^{-c_C}}{!} Y \frac{Y^1 Z}{dh_k W(h_k)} \frac{Z}{dx(x)}}{= 0 = 1 \sum_{k=1}^p} + \frac{1}{2} \sum_s \log G_s^R(x; fh_k g) \log(2 \cosh((h_k))) + O(n^2) \quad (32)$$

with

$$G_s^R(x; fh_k g) = \frac{X}{e^{(x + J_0 s)}} \frac{Y}{e^{(p-1) \sum_{k=1}^{p-1} h_k}} \frac{X}{e^{p \sum_{k=1}^{p-1} h_k + \frac{J}{c}}} \quad (33)$$

So the largest eigenvalue  $\lambda_0$  is equal to 1 in the limit  $n \rightarrow 0$ .

### C. Thermodynamics

We can now evaluate the free energy of the system. Starting from (7) and (15) we arrive at

$$f(\beta) = \frac{c(1-p)}{p} \sum_{k=1}^p \frac{Y^p Z}{dh_k W(h_k)} \frac{\#^2 0}{4 \log \beta} \sum_{k=1}^p \frac{X}{e^{p \sum_{k=1}^p h_k + \frac{J}{c}}} + \log \beta \sum_{k=1}^p \frac{X}{e^{p \sum_{k=1}^p h_k + A}} + \frac{X}{2} \frac{e^{-c_C}}{!} Y \frac{Y^1 Z}{dh_k W(h_k)} \frac{Z}{dx(x)} + \frac{1}{2} \sum_s \log G_s^R(x; fh_k g) \log(2 \cosh((h_k))) \quad (34)$$

which is the final result. In this expression the Poisson distribution  $\frac{e^{-c_C}}{!}$  of mean  $c$  can be clearly associated to the degree distribution of the graph. Once a degree has been sampled from this distribution, one performs integrals over the densities  $fh_k g$  and one over  $dx(x)$ . Thus we can think of the  $fh_k g$  as the distribution of effective fields coming from the long-range connections and  $dx(x)$  as those coming from the ring.

The order parameters of the system under study are the average magnetization which reads, recalling Eq. (26)

$$m = \frac{1}{N} \sum_i \frac{X}{Z} \quad (35)$$

$$= \frac{X}{Z} \frac{1}{N} \sum_i \frac{X}{Z} \frac{dh W(h)}{dh W(h)} \frac{Y^n}{=1} \frac{e^{h_i}}{2 \cosh(h)} \quad (36)$$

$$\stackrel{RS}{=} \frac{dh W(h)}{dh W(h)} \tanh(h) \quad (37)$$

and the Edwards-Anderson parameter function

$$q = \frac{1}{N} \sum_i \frac{X}{Z} \frac{!}{i} \quad ; \quad \epsilon \quad (38)$$

$$= \frac{X}{Z} \frac{1}{N} \sum_i \frac{X}{Z} \frac{dh W(h)}{dh W(h)} \frac{Y^n}{=1} \frac{e^{h_i}}{2 \cosh(h)} \quad (39)$$

$$\stackrel{RS}{=} \frac{dh W(h)}{dh W(h)} \tanh^2(h) \quad (40)$$

We remark that due to the RS assumption  $m = m$  for  $x$ ,  $q = q$  for  $y$  &  $z$ , and  $q = 1$ .

Next, in order to obtain the phase diagram we have to study the solutions of the self-consistent equations (29), (30) and (31). It is easily seen that theeld-distributions  $(x) = (y) = W(x) = (x)$  are a solution of these equations, corresponding to the paramagnetic phase according to Eq. (37). For high temperatures, this is the only solution present. Following a standard procedure in finite-connectivity theory (see, e.g. [7]) we discuss continuous bifurcations away from this solution in order to find (second-order) phase transitions. Since we are dealing witheld-distributions this means that theelds will be narrowly distributed around zero so that we can expand the equations (37) and (40), using equation (31). In order to quantify the difference with the delta-peak-solution we assume  $dh h^k (h) = O(k)$  and  $dh h^k (h) = O(k)$  with  $j \geq 1$  such that

$$m = \frac{Z}{Z} = \frac{dx}{dx} (x) x + \frac{dy}{dy} (y) y + O(3) \quad (41)$$

$$q = \frac{Z}{Z} = \frac{dx^2}{dx dy} (x) (y) (x + y)^2 + O(3) \quad (42)$$

So in order to find the transition towards non-zero magnetization we look for bifurcations where the first moments become of order  $1$ . Introducing  $\bar{x} = dx x / (x)$  and  $\bar{y} = dy y / (y)$ , and recalling Eqs. (29) and (30) we find the following set of self-consistent equations

$$\bar{x} = \bar{x} \tanh(J_0) + c \tanh\left(\frac{J}{c}\right) \frac{(\bar{x} + \bar{y})^{p-1}}{J} \quad (43)$$

$$\bar{y} = \bar{y} \tanh(J_0) + c \tanh(J_0) \tanh\left(\frac{J}{c}\right) \frac{(\bar{x} + \bar{y})^{p-1}}{J} \quad (44)$$

For  $p > 2$  the second terms in the r.h.s. of these equations are of a higher order in  $c$  and, hence, no second-order bifurcations to a ferromagnetic phase are found. For  $p = 2$  these equations do lead to a second-order bifurcation at

$$1 = c \tanh\left(\frac{J}{c}\right) \frac{\exp(2J_0)}{J} \quad (45)$$

in agreement with [7].

Analogously, we can look for bifurcations to a spin-glass transition by expanding the second-order moments, assuming that  $\bar{x} = \bar{y} = 0$ . Introducing  $\bar{x}^2 = dx x^2 / (x)$  and  $\bar{y}^2 = dy y^2 / (y)$  we get

$$\bar{x}^2 = \bar{x}^2 \tanh^2(J_0) + c \tanh^2\left(\frac{J}{c}\right) \frac{(\bar{x} + \bar{y})^{2(p-1)}}{J} \quad (46)$$

$$\bar{y}^2 = \bar{y}^2 \tanh^2(J_0) + c \tanh^2(J_0) \tanh^2\left(\frac{J}{c}\right) \frac{(\bar{x} + \bar{y})^{2(p-1)}}{J} \quad (47)$$

Again, from this we can deduce that there is no second-order spin-glass transition for  $p > 2$  but for  $p = 2$  a continuous bifurcation to  $q > 0; m = 0$  occurs at

$$1 = c \tanh^2\left(\frac{J}{c}\right) \frac{\cosh(2J_0)}{J} \quad (48)$$

The  $p = 2$ -results are in agreement with those of [7], where it is also argued that for  $J; J_0 \rightarrow 0$  the second-order paramagnetic to spin-glass instability cannot occur as it will always be preceded by the ferromagnetic one when lowering the temperature. From simulation experiments we find some evidence for glassy behavior at lower temperatures for all  $p$ , especially for  $J_0 = 0$ , as will be shortly discussed in Section V. There we also study first-order transitions by employing the transfer-matrix analysis developed in Sec. IIIA, IIIB together with population dynamics.

#### IV . THE 1 + 1 MODEL

A limiting case of the previous results is an Ising chain superimposed on a fully connected hypergraph. This model gets a mean-field character and can be solved analytically by using the transfer-matrix approach.

In order to have a multispin interaction between every multiplet of  $p$  spins we must take  $c = N^{p-1} = (p-1)!$  (See e.g. equation (1)). Recalling the Hamiltonian (5) and the local field (6) this leads to the following free energy

$$f = \lim_{N \rightarrow 1} \frac{1}{N} \log \text{Tr} \exp \left( \frac{J}{pN^{p-1}} \sum_{j_1, j_2, \dots, j_p} X_{j_1, j_2, \dots, j_p} + J_0 \sum_{i, i+1} A_i A_{i+1} \right) \quad (49)$$

$$= \lim_{N \rightarrow 1} \frac{1}{N} \log \text{Tr} \sum_m dm dm \exp \left( \frac{1}{N} \sum_i X_i \right) \exp \left( \frac{JN}{p} m^p + J_0 \sum_i X_i \right) \quad (50)$$

$$= \lim_{N \rightarrow 1} \frac{1}{N} \log \sum_m dm dm \exp \left( \frac{JN}{p} m^p \right) \text{Tr} T^N \quad : \quad (51)$$

where we have introduced the magnetization order parameter

$$Z = \sum_m \left( \frac{1}{N} \sum_i X_i \right) \quad (52)$$

Here  $T$  is the transfer matrix

$$T = \begin{pmatrix} e^{im + J_0} & e^{im - J_0} \\ e^{im - J_0} & e^{im + J_0} \end{pmatrix} \quad (53)$$

The eigenvalues of this matrix are

$$(m) = e^{J_0} \cosh(im) - e^{2J_0} \cosh^2(im) - 2 \sinh(2J) \quad (54)$$

Using the fact that  $\text{Tr} T^N = \sum_{m=+}^N \sum_{i=1}^N$  we write equation (51) as

$$f = \lim_{N \rightarrow 1} \frac{1}{N} \log \sum_m dm dm \exp \left( \frac{JN}{p} m^p + N \log \left( \frac{m}{+} \right) \right) \quad (55)$$

In the limit  $N \rightarrow 1$ , the fixed-point equation minimizing the free energy is given by

$$m = \frac{\sinh(Jm^{p-1})}{\sinh^2(Jm^{p-1}) + e^{-4J_0}} \quad (56)$$

We remark that this equation reduces to the one presented in [18] for  $p = 2$ .

To find the phase diagram of this system we perform a bifurcation analysis. It is easy to see that  $m = 0$ , indicating the paramagnetic phase, satisfies Eq. (56). To find second-order transitions bifurcating continuously from the paramagnetic solution, we put the derivative of the r.h.s of (56) equal to one at  $m = 0$ . We immediately observe that there are no solutions for  $p > 2$ , but for  $p = 2$  we find the solution

$$J = e^{-2J_0} \quad (57)$$

To look for first-order transitions we have to find out where the derivative mentioned above is equal to one for a non-zero  $m$ , together with equation (56). In this model this can be done analytically by introducing the parametrization

$$x = Jm^{p-1}; \quad x \in [-1, 1] \neq 0 \quad (58)$$

leading to

$$J_0(x) = \frac{1}{4} \log \frac{\tanh(x) \sinh^2(x)}{x(p-1) \tanh(x)} \quad (59)$$

$$J(x) = x \frac{x(p-1)}{x(p-1) \tanh(x)}^{\frac{1}{2}(p-1)} \quad (60)$$

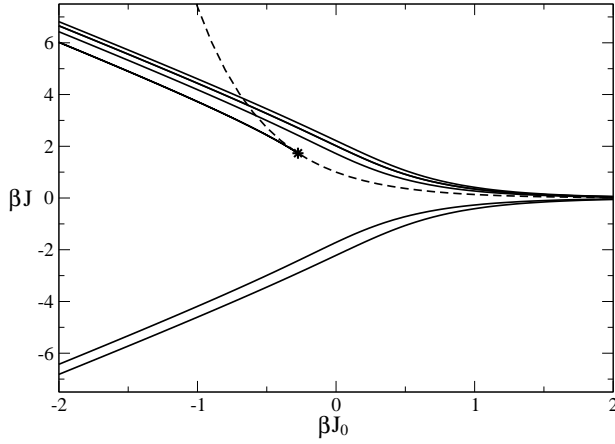


FIG. 2: Phase diagram for the 1+1 model in the  $J - J_0$  plane for different  $p$ . The solid lines indicate first-order transitions: for  $J > 0$ ,  $p = 2; 3; 4; 5$  from bottom to top, and for  $J < 0$ ,  $p = 3; 5$  from top to bottom. The dashed line is the second-order transition line for  $p = 2$ . The star indicates the tricritical point for  $p = 2$ .

We remark that in the limit  $x \rightarrow 1$ , the slope of  $J = J_0$  approaches 2 and, hence, is  $p$ -independent.

For any non-zero  $x$  we can now find a couple  $J$  and  $J_0$  at which a first order phase transition occurs. The value of the magnetization  $m$  at that point is given by equation (58). These phase transition lines are plotted in Fig. 2 for several values of the degree  $p$ .

We see that no transitions occur for even  $p$  and  $J < 0$ . Furthermore, we remark the  $J$  symmetry for odd  $p$ . The ferromagnetic phase is situated to the right of the transition lines, so for odd  $p$  the paramagnetic phase is in between the symmetrical solid lines, for  $p$  even it lies below the corresponding solid line. For increasing  $p$ , the ferromagnetic region decreases. For the special case of  $p = 2$  the paramagnetic and ferromagnetic phase coexist between the first and second-order transition lines with a tricritical point  $J = \frac{1}{3} \approx 1.732$ ;  $J_0 = \log(3) \approx 4.0275$ . The latter results are in agreement with the results of [18] and with those of [19] in the case of one dimension.

## V. RESULTS FOR FINITE $c$ .

The main equations describing the thermodynamics of the small-world hypergraph for finite  $c$  are Eqs. (29), (30) and (31). To solve these equations we use the population dynamics algorithm to generate field distributions together with Monte Carlo integration over the generated populations in order to obtain the physical parameters. The important parameters of this algorithm are the size of the populations and the number of iterations. The size of the populations has to be big enough to get clearly outlined distributions keeping in mind, however, that the computational time required for the algorithm to converge is linear in this parameter. In most cases we find that populations of 10000 fields give accurate results. The number of iterations per spin depends strongly on the physical parameters. It turns out that most of the time about 1000 iterations results in a reasonable accuracy.

From the 1+1 model solved analytically in Section IV we learn already that the physics for  $p = 2$  versus the one for  $p = 3$  might be very different. As a benchmark test for our derivations we have reproduced some of the results for  $p = 2$  found in [7, 19]. We do not repeat them here but concentrate on  $p = 3$  in the sequel.

For initial conditions that give rise to an initial magnetization close to one, the population dynamics algorithm evolves to a zero or non-zero final magnetization, indicating a phase transition. This transition again appears to be first order, and located at the same point as the transition to non-zero  $q$ . First we calculate, for general  $p$ , the critical temperatures at which this phase transition occurs. They are plotted in Fig. 3 in the case  $p = 3; 4$  for the model without chain contribution ( $J_0 = 0$ ). Above the transition line we find the paramagnetic phase, below the ferromagnetic phase. For numerical reasons we have only considered  $T = 0.005$ . The results for  $p = 3$  are in agreement

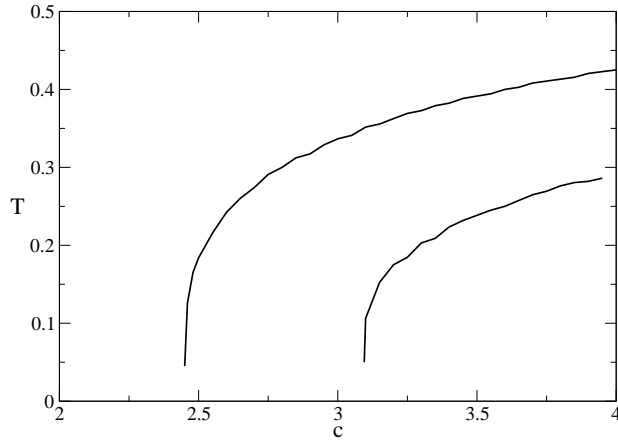


FIG. 3: Critical temperatures as a function of the average connectivity  $c$  for the ferromagnetic-paramagnetic phase transition in the model without chain contribution ( $J_0 = 0$ ): from top to bottom  $p = 3; 4$ .

with the  $T_{fm}$  transition line given in [13].

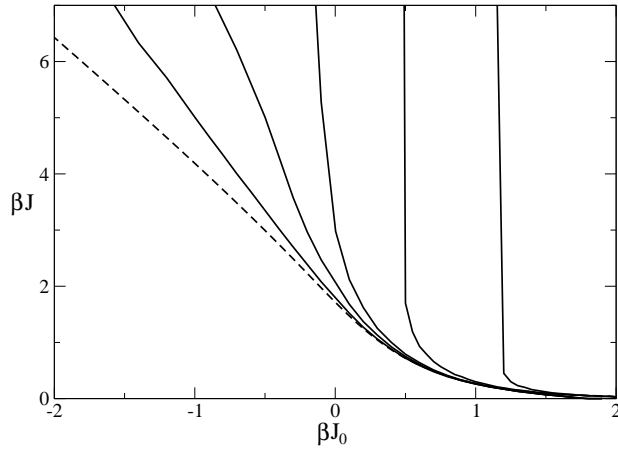


FIG. 4: Phase transition lines in the  $J - J_0$  plane for  $p = 3$  and different connectivities  $c$ : solid lines from right to left  $c = 0.25; 1; 3; 6; 20$ , the dashed line is for  $c = 1$ .

Furthermore, we search for the transition lines in the  $J - J_0$  plane. These transitions between ferromagnetic and paramagnetic behavior are plotted in Fig. 4 for  $p = 3$  and  $c = 0.25; 1; 3; 6; 20$  (solid lines), together with the theoretical result for  $c = 1$  (dashed line). The latter model is solved analytically in Section IV. All transitions shown here are first-order. The ferromagnetic phase is situated at the right of the transition lines and increases substantially with growing  $c$ . For smaller values of  $c$  the curves become vertical indicating the critical values of  $J_0$  below which no order is possible. For bigger values of  $c$ , the transitions approach the analytically derived  $c = 1$  result. Just as in the  $p = 2$  case, the small-world hypergraph has its ferromagnetic transition at finite temperatures for all non-zero values of  $c$ .

Simulations have been performed for this small-world model with Glauber dynamics. As a typical example the results for  $p = 3; c = 3$  are plotted in Fig. 5 for  $10^4$  spins and different number of iterations. Very good agreement with the population dynamics solution of the replica-symmetric transfer matrix analysis is found in the positive  $J_0$

region.

When  $J_0$  is negative, however, the relaxation time of the system increases tremendously due to domain tipping, and no good agreement is reached with the population dynamics results for up to  $5 \times 10^6$  iterations per spin. This is an example of critical slowing down near the transition line. The simulations show some further evidence for glassy dynamics (very large spin-spin autocorrelation times) for lower temperatures. In principle, this can be understood since the very sparse system contains two anti-ferromagnetic bonds per spin coming from the chain and, in average,  $c$  (of order  $O(1)$ ) ferromagnetic bonds from the graph. A detailed discussion of this non-trivial glassy behavior is beyond the scope of the present work.

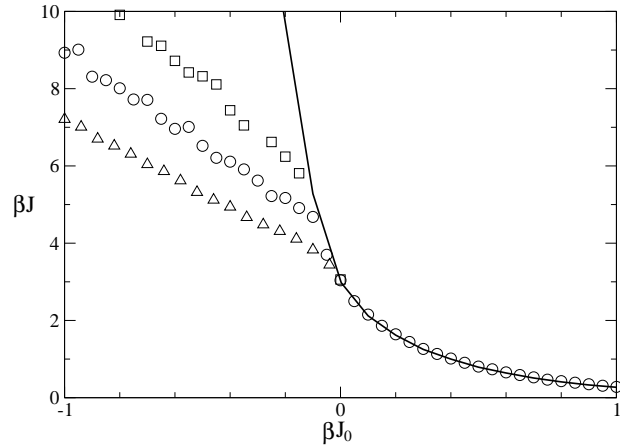


FIG. 5: Phase transition lines in the  $J \rightarrow J_0$  plane for  $p = 3; c = 3$ . The solid line represents the population dynamics result. The triangles, circles and squares indicate the results of simulations with  $10^4$  spins and, respectively,  $2000; 5 \times 10^4; 5 \times 10^6$  iterations per spin.

## V I. DISCUSSION

In this paper, we have studied the thermodynamics of small-world hypergraphs consisting of sparse Poisson random graphs with  $p$ -spin interactions superimposed onto a one-dimensional Ising chain with nearest-neighbor interactions. Using a replica-symmetric transfer-matrix analysis and the population dynamics algorithm we have obtained the phase behavior of this system as a function of the short-range and long-range couplings and the average long-range connectivity. In contrast with  $p = 2$  we find that all paramagnetic-ferromagnetic phase transitions are purely first order. For fixed  $p$  and increasing connectivity the ferromagnetic phase increases substantially and the transition line converges to the analytically derived result for the  $1+1$  model. For the latter the ferromagnetic region decreases for growing  $p$ . Using a bifurcation analysis we see that again,  $p = 2$  also has a second-order transition and the first-order transition occurs only for  $J_0 = 0.275$ .

Extensive simulations on this model have been performed using Glauber dynamics. Very good agreement with the population dynamics results have been obtained for ferromagnetic chain couplings. For anti-ferromagnetic chain couplings, the dynamics slows down tremendously and glassy behavior is seen in this region. A detailed discussion of this behavior and an exact determination of the corresponding transition line is non-trivial and left for future work.

## Acknowledgments

We would like to thank Heinz Humer for interesting discussions. This work is partially supported by the Fund for Scientific Research Flanders-Belgium.

Appendix: self-consistent equation for  $\langle x \rangle$ 

In order to derive the self-consistent equation for  $\langle x \rangle$  we insert (27) into the l.h.s. of (22) using (19)

$$\begin{aligned} & X \\ & T ; \quad \mathbb{E} \ln_0( ) \\ & = \frac{X}{\exp^0} \frac{X}{J_0} + C \frac{X}{F(k)} e^{\frac{J}{c} p} \frac{1}{1 \dots p-1} \frac{1}{1 A} \frac{Z}{dx} \langle x \rangle e^{\frac{p}{c} n-1} \quad (61) \end{aligned}$$

$$= \frac{X}{dx} \frac{Z}{\langle x \rangle e^{\frac{p}{c} n-1}} e^{\frac{p}{J_0}} \frac{0}{e^c} \frac{0}{\frac{C}{A} \frac{1}{1}} \frac{X}{F(k)} e^{\frac{J}{c} p} \frac{1}{1 \dots p-1} \frac{1}{A} \frac{1}{A} \quad (62)$$

$$= \frac{Y^n}{dx} \frac{X}{\langle x \rangle e^{\frac{p}{c} n-1}} \frac{Z}{J_0} \frac{!}{X} \frac{0}{\frac{B}{A} \frac{e^c}{!}} \frac{X}{F(k)} e^{\frac{J}{c} p} \frac{1}{1 \dots p-1} \frac{1}{A} \frac{1}{A} \quad (63)$$

In the transition to (62) we have used that  $F( )$  is normalized to separate the term  $e^c$ . We then have expanded the outermost of the remaining double exponential into a series. In (63) we have written the powers as a product over a new replica index  $\alpha$ . The vectors now have two replica indices. We also note that a poissonian factor appears. At this point we insert Eq. (26) to obtain

$$\begin{aligned} & X \\ & T ; \quad \mathbb{E} \ln_0( ) = \frac{Y^n}{dx} \frac{X}{\langle x \rangle e^{\frac{p}{c} n-1}} \frac{Z}{J_0} \frac{!}{\frac{1}{0}} \\ & = \frac{1}{0} \frac{X}{\frac{B}{A} \frac{e^c}{!}} \frac{X}{Y} \frac{Y}{Z} \frac{dh_k}{dh_k} \frac{W(h_k)}{2 \cosh(h_k)} \frac{Y^n}{\frac{1}{2} \cosh(h_k)} \frac{\frac{e^{h_k}}{h_k} \frac{!}{k}}{e^{\frac{J}{c} p} \frac{1}{1 \dots p-1}} \frac{1}{A} \\ & = \frac{X}{\frac{B}{A} \frac{e^c}{!}} \frac{Y}{Y} \frac{Y}{Z} \frac{dh_k}{dh_k} \frac{W(h_k)}{(2 \cosh(h_k))^n} \frac{Z}{dx} \langle x \rangle \frac{!}{\frac{1}{0}} \\ & = \frac{Y^n}{\frac{1}{0}} \frac{X}{e^{(x+J_0)}} \frac{Y}{\frac{1}{1 \dots p-1}} \frac{X}{e^{\frac{p}{c} \frac{1}{k=1} h_k k + \frac{J}{c} 1 \dots p-1}} \frac{A}{A} \quad (64) \end{aligned}$$

We now focus on the second line of the last equation

$$\begin{aligned} & \frac{Y^n}{\frac{1}{0}} \frac{X}{e^{(x+J_0)}} \frac{Y}{\frac{1}{1 \dots p-1}} \frac{X}{e^{\frac{p}{c} \frac{1}{k=1} h_k k + \frac{J}{c} 1 \dots p-1}} \\ & = \exp \frac{X^n}{\log G^R(x; fh_k g)} \frac{!}{\frac{1}{1}} \\ & = \exp \frac{X^n}{\frac{1}{2} (1+s) \log G_s^R(x; fh_k g)} \frac{!}{\frac{1}{s=1}} \\ & = \exp \frac{1}{2} \frac{X}{s \log G_s^R(x; fh_k g)} \frac{X^n}{\frac{1}{s=1}} + \frac{n}{2} \frac{X}{\log G_s^R(x; fh_k g)} \frac{!}{\frac{1}{s=1}} \quad (65) \end{aligned}$$

with (recall equation (33))

$$G^R(x; fh_k g) = \frac{X}{e^{(x+J_0)}} \frac{Y}{\frac{1}{1 \dots p-1}} \frac{X}{e^{\frac{p}{c} \frac{1}{k=1} h_k k + \frac{J}{c} 1 \dots p-1}} \quad (66)$$

We take the limit  $n \rightarrow 0$  in (65) and replace the last line of (64) with this limit

$$\begin{aligned}
 X \quad T, \quad F[u_0] &= \frac{X^{\frac{1}{2}}}{!} \frac{e^{\frac{c}{C}}}{!} \frac{Y^{\frac{1}{2}}}{=1} \frac{Z^{\frac{1}{2}}}{k=1} \frac{dh_k}{!} \frac{W(h_k)}{(2 \cosh(h_k))^n} \frac{\#}{dx} (x) \\
 &= \frac{\exp \frac{1}{2} X}{dx^0} \frac{s \log G_s^R(x; fh_k g)}{s=1} \frac{X^n}{=1} \\
 &= \frac{Z}{dx^0} \frac{X^{\frac{1}{2}}}{!} \frac{e^{\frac{c}{C}}}{!} \frac{Y^{\frac{1}{2}}}{=1} \frac{Z^{\frac{1}{2}}}{k=1} \frac{dh_k}{!} \frac{W(h_k)}{(2 \cosh(h_k))^n} \frac{\#}{dx} (x) \\
 &= \frac{x^0}{!} \frac{1}{2} \frac{X}{s=1} \frac{s \log G_s^R(x; fh_k g)}{exp} \frac{X^n}{=1} \quad (67)
 \end{aligned}$$

This expression is now of the form (27) and identifying terms leads to

$$u(x^0) = \frac{X^{\frac{1}{2}}}{!} \frac{e^{\frac{c}{C}}}{!} \frac{Y^{\frac{1}{2}}}{=1} \frac{Z^{\frac{1}{2}}}{k=1} \frac{dh_k}{!} \frac{W(h_k)}{dx} (x) \quad x^0 \quad \frac{1}{2} \frac{X}{s=1} \frac{s \log G_s^R(x; fh_k g)}{!} \quad (68)$$

where we have used additionally that  $(2 \cosh(h_k))^n \rightarrow 1$  when  $n \rightarrow 0$ .

This equation can be simplified further as follows

$$\begin{aligned}
 G_s^R(x; fh_k g) &= \frac{X}{!} \frac{e^{(x+J_0)}}{=} \frac{Y}{=1} \frac{X}{1} \frac{e^{\sum_{k=1}^{p-1} h_k}}{1 \dots p-1} \\
 &= 4 \cosh(x+J_0) \frac{Y}{=1} \frac{X}{2 \dots p-1} \cosh(h_1 + \frac{J}{C}) \frac{e^{\sum_{k=2}^{p-1} h_k}}{1 \dots p-1} \\
 &= 4 \exp \frac{1}{2} \log(\cosh(h_1 + \frac{J}{C}) \cosh(h_1 - \frac{J}{C})) \cosh(x+J_0) \\
 &= \frac{Y}{=1} \frac{X}{2 \dots p-1} \exp \frac{1}{2 \dots p-1} \operatorname{atanh}(\tanh(h_1) \tanh(\frac{J}{C})) \frac{e^{\sum_{k=2}^{p-1} h_k}}{1 \dots p-1} \\
 &= C(h_1; h_2; \dots; h_{p-1}; J) \exp \frac{X}{=1} \operatorname{atanh} \frac{\tanh(\frac{J}{C})}{k=1} \frac{Y^{\frac{1}{2}}}{k=1} \tanh(h_k) \quad (68)
 \end{aligned}$$

with  $C(h_1; h_2; \dots; h_{p-1}; J)$  a function depending only on  $h_1; h_2; \dots; h_{p-1}; J$  and  $C$ . We finally arrive at

$$\begin{aligned}
 &\frac{1}{2} \frac{X}{s=1} \frac{s \log G_s^R(x; fh_k g)}{!} \\
 &= \frac{1}{2} \frac{X}{=1} \operatorname{atanh} \frac{\tanh(\frac{J}{C})}{k=1} \frac{Y^{\frac{1}{2}}}{k=1} \tanh(h_k) + \operatorname{atanh}(\tanh(x) \tanh(J_0)) \quad (69)
 \end{aligned}$$

In this way we have obtained the self-consistent equation (29) for  $(x)$ . The equation for  $(x)$  can be derived in an analogous way.

From these equations we can also find the largest eigenvalue  $\lambda_0$ . Keeping the factor of order  $n$  in (65) we end up with the following equation

$$\begin{aligned}
 u_0(x^0) &= \frac{X^{\frac{1}{2}}}{!} \frac{e^{\frac{c}{C}}}{!} \frac{Y^{\frac{1}{2}}}{=1} \frac{Z^{\frac{1}{2}}}{k=1} \frac{dh_k}{!} \frac{W(h_k)}{(2 \cosh(h_k))^n} \frac{\#}{dx} (x) \\
 &= \frac{x^0}{!} \frac{1}{2} \frac{X}{s=1} \frac{s \log G_s^R(x; fh_k g)}{exp} \frac{X}{s=1} \frac{\frac{n}{2} \log G_s^R(x; fh_k g)}{!} \quad (70)
 \end{aligned}$$

When we integrate both sides over  $x^0$  and expand the last exponential we find equation (32).

---

- [1] A. Pekalski, *Phys. Rev. E* 64, 057104 (2001).
- [2] M. Givan and M. E. J. Newman, *Proc. Natl. Acad. Sci. U.S.A.* 99, 7821 (2002).
- [3] L. Siming et al, *Science* 303, 540 (2004).
- [4] A.-L. Barabasi and Z. N. Oltvai, *Nat. Rev. Gen.* 5, 101 (2004).
- [5] M. E. J. Newman, *Proc. Natl. Acad. Sci. U.S.A.* 98, 404 (2002).
- [6] A. Barrat and M. Weigt, *Eur. Phys. J. B* 13, 547 (2000).
- [7] T. N.ikoletopoulos, A. C. C. Coolen, I. Perez Castillo, N. S. Skantzos, J. P. L. Hatchett and B. Wemmenhove, *J. Phys. A: Math. Gen.* 37, 6455 (2004).
- [8] R. Albert and A.-L. Barabasi, *Rev. Mod. Phys.* 74, 47 (2002).
- [9] M. E. J. Newman, *SIAM Rev.* 45, 167 (2003).
- [10] Duncan J. Watts, *Small Worlds: The Dynamics of Networks between Order and Randomness* (Princeton University Press, Princeton, 2003).
- [11] S. N. Dorogovtsev and J. F. F. Mendes, *Evolution of Networks: From Biological Networks to the Internet and WWW* (Oxford University Press, London, 2003).
- [12] A.-L. Barabasi, *Linked: The New Science of Networks* (Oxford University Press, London, 2002).
- [13] S. Franz, M. M. Mezard, F. Ricci-Tersenghi, M. Weigt, and R. Zecchina, *Europhys. Lett.* 55, 465 (2001).
- [14] A. Barrat and R. Zecchina, *Phys. Rev. E* 59, 1299 (1999).
- [15] F. Ricci-Tersenghi, M. Weigt and R. Zecchina, *Phys. Rev. E* 63, 026702 (2001).
- [16] R. Heylen, N. S. Skantzos, J. Busquets Banco and D. Bolle, *Phys. Rev. E* 73, 016138 (2006).
- [17] M. M. Mezard and G. Parisi, *Eur. Phys. J. B* 20, 217 (2001).
- [18] N. S. Skantzos and A. C. C. Coolen, *J. Phys. A: Math. Gen.* 33, 5785 (2000).
- [19] M. Kardar, *Phys. Rev.* 28, 244 (1983).
- [20] M. M. Mezard, G. Parisi and M. A. Virasoro, *Spin Glass Theory and Beyond* (World Scientific, Singapore, 1987).